Detection of Multiple Primary Systems Using DAA UWB-IRs

Serhat Erküçük,[1] Lutz Lampe,[2] and Robert Schober[2]
[1]Department of Electronics Engineering, Kadir Has University, Istanbul, Turkey
[2]Department of Electrical and Computer Engineering, University of British Columbia, Vancouver, BC, Canada
E-mail: {serkucuk}@khas.edu.tr, {lampe, rschober}@ece.ubc.ca

***Abstract*— Underlay ultra wideband (UWB) systems have to be able to detect the presence of primary systems operating in the same band for detect-and-avoid (DAA) operation. In this paper, the performances of joint and independent detection of multiple primary systems are investigated assuming that the primary systems are potentially dependent (e.g., frequency division duplex uplink-downlink communications). Joint detection is performed based on generating the maximum a posteriori (MAP) decision variables at the receiver, where some bias terms are used with these variables in order to achieve a desired trade-off between the detection and false alarm probabilities. Independent detection is performed based on the Neyman-Pearson (NP) test, which optimizes system threshold values individually in order to achieve the best detection probability for a given false alarm probability value. When the two detection schemes are compared, it is shown that the gain of joint detection depends on the joint system activity values and the considered receiver operating characteristic (ROC) region, where the complementary ROC curves illustrate the trade-off between missdetection and false alarm probabilities.**

I. Introduction

Ultra wideband (UWB) systems are designed as underlay systems to share the spectrum with existing licensed communications systems. Despite the low transmission power of such underlay systems, regulatory agencies in Europe and Japan have made the implementation of detect-and-avoid (DAA) techniques mandatory in some bands to avoid interference to existing systems. In any DAA scheme, the first step is *spectrum sensing* in order to assess whether there is an active primary system in the common band or not. For low-rate UWB impulse radios (UWB-IRs), which are based on the IEEE 802.15.4a standard [1] and have non-coherent receiver structures, energy detection is the conventional method to decide on the presence of a primary system.

Energy detection of primary systems has been investigated in the context of both cognitive radios [2], [3] and UWB-IRs [4], [5]. The common approach of these methods is the detection of a primary system in a single frequency band and the improvement of the detection performance via cooperative techniques such as using multiple antennas, multiple observations, and time-domain diversity schemes. While such cooperative techniques are necessary to achieve a high level of signal detection reliability, signal detection in a single frequency band should be extended to multiple bands if multiple licensed systems are active within the bandwidth of a UWB system. Similarly, it is more practical for a cognitive radio to assess the presence of multiple spectrum holes.

The literature on energy detection in multiple frequency bands is rather limited compared to energy detection in a single band. In [6], we have studied the energy detection of multiple primary systems operating in the same frequency band with UWB-IRs, where each system was assumed to access the channel independently. In addition to formulating the false alarm and detection probabilities, we evaluated the percentages of time the UWB-IR system operated usefully and harmfully (causing interference to primary systems). In [7] and [8], the authors have considered multiband joint detection for cognitive radios and have maximized the aggregate opportunistic throughput over multiple bands subject to some constraints on the amount of interference to primary users. The common assumption in [6]–[8] is that the primary systems in different bands are independent. However, in a realistic scenario the licensed systems in different bands may be dependent; e.g., the presence of an active uplink could possibly mean there is also an active downlink.

In this paper, we investigate the potential advantages of joint detection of multiple primary systems over independent detection assuming that these systems are dependent and their dependence statistics are available. Accordingly, for joint detection the maximum a posteriori (MAP) decision variables are generated at the receiver, where each variable is associated with a bias term in order to achieve a desired trade-off between detection and false alarm probabilities. This is illustrated by the complementary receiver operating characteristic (ROC) curves. Independent detection is performed based on the Neyman-Pearson (NP) test, which optimizes system threshold values individually in order to achieve the best detection probability for a given false alarm probability value. The comparison of the two detection schemes shows that the gain of joint detection depends on the joint system activity values and the considered ROC region.

The rest of the paper is organized as follows. In Section II, the primary system signalling structure and the UWB-IR receiver structure are introduced. In Section III, independent

This work was supported in part by the National Sciences and Engineering Research Council (NSERC) of Canada under Grant STPSC 364995.

detection based on the NP test and joint detection based on the MAP criterion are presented. In Section IV, analysis and simulation results are presented in order to compare the detection methods. Concluding remarks are given in Section V.

II. System Model

In this section, we assume the presence of M Orthogonal Frequency Division Multiplexing (OFDM)-based systems with possibly different transmission bandwidths coexisting with a UWB-IR system in the same frequency band. To determine the presence or absence of the primary systems, the UWB-IR system uses tunable bandpass filters to eliminate the out-of-band noise before performing energy detection in the desired bands. In the next three subsections, the primary system signal model and the UWB-IR receiver model are explained, and the hypotheses are defined.

A. OFDM-based Signal Model

For the primary system, WiMAX-OFDM is considered as defined in [9]. Accordingly, the signal of the mth WiMAX system, where $m \in \{1, 2, \ldots, M\}$, is given by

$$s_m(t) = \sum_{l=-\infty}^{\infty} \sum_{k=0}^{K-1} a_{m,k,l}\; p_k(t - lT_s)\, e^{j2\pi f_m t} \tag{1}$$

where $p_k(t) = \frac{1}{\sqrt{T_d}} e^{j2\pi\Delta_m k(t-T_c)}$, $t \in [0, T_s]$, is the basis function for subcarrier k, K is the number of subcarriers, T_s, T_d, and T_c are the symbol, data, and prefix durations, respectively, and f_m is the carrier frequency of the mth system. The bandwidth per subcarrier is $\Delta_m = W_m/K$, where W_m is the transmission bandwidth. The information symbol for the lth symbol and kth subcarrier of the mth system, $a_{m,k,l}$, can be modulated with either binary phase-shift keying (BPSK), quaternary PSK (QPSK), 16-ary quadrature amplitude modulation (16-QAM) or 64-QAM.

B. UWB-IR Receiver Model

It is assumed that the UWB-IR system has prior knowledge of the carrier frequencies and transmission bandwidths of the primary systems, and uses ideal zonal bandpass filters, $h_{ZF,m}(t)$, before energy detection. Accordingly, the signal received in the mth frequency band after filtering is given by

$$r_m(t) = A_m\, e^{j\theta_m}\, s_m(t - \tau_m) + n_m(t), \quad 1 \le m \le M, \tag{2}$$

where each WiMAX signal passes through a channel with amplitude A_m and phase θ_m uniformly distributed over $[0, 2\pi)$, τ_m is the timing offset between the two systems, and $n_m(t)$ is the band-limited additive white Gaussian noise (AWGN) with variance $\sigma^2_{n_m} = N_0 W_m$. Using a square-law detector and normalizing the output with the two-sided noise power spectral density $N_0/2$, the decision variable for the mth system can be obtained as

$$d_m = \frac{2}{N_0} \int_0^{T_m} |r_m(t)|^2\, dt \tag{3}$$

where T_m is the integration time for the mth system and $|\cdot|$ is the absolute value operator. Adopting the sampling theorem approximation used for bandpass signals in [2] and [10], the decision variable can be approximated as

$$d_m \approx \frac{1}{N_0 W_m} \sum_{i=1}^{T_m W_m} \Big[(A_c s_{ci} - A_s s_{si} + n_{ci})^2 + (A_c s_{si} + A_s s_{ci} + n_{si})^2 \Big] \tag{4}$$

where s_{ci} and n_{ci} are the in-phase, and s_{si} and n_{si} are the quadrature components of $s_m(t-\tau_m)$ and $n_m(t)$, respectively, sampled at the Nyquist rate, $A_c = A_m \cos\theta_m$, and $A_s = A_m \sin\theta_m$.

C. Hypotheses and Decision Variable

We now define two hypotheses, $H_{0,m}$ and $H_{1,m}$, referring to the absence and presence of the signal of the mth primary system as

$$H_{0,m}: \quad r_m(t) = n_m(t) \tag{5}$$

$$H_{1,m}: \quad r_m(t) = A_m\, e^{j\theta_m}\, s_m(t - \tau_m) + n_m(t). \tag{6}$$

Under $H_{0,m}$, it can be shown based on (4) that d_m has a χ^2 distribution with $N_m = 2T_m W_m$ degrees of freedom (DOF) and variance $\sigma^2_m = \frac{\sigma^2_{n_m}}{N_0 W_m} = 1$. Under $H_{1,m}$, based on the central limit theorem, the samples of a WiMAX-OFDM signal given in (4) for a large number of subcarriers K sampled at the Nyquist rate can be approximated as independent and identically distributed (i.i.d.) zero mean Gaussian random variables. Accordingly, when the primary system is active, d_m has a χ^2 distribution with $N_m = 2T_m W_m$ DOF and variance $\sigma^2_m = \gamma_m + 1$, where $\gamma_m = \frac{A_m^2 \sigma_s^2}{N_0 W_m}$ is the signal-to-noise ratio (SNR), σ_s^2 is the variance of the WiMAX signal samples, and the term "1" is due to the normalized noise samples. Thus, the probability density function (pdf) of d_m for either hypothesis can be expressed as

$$f_{D_m}(d_m) = \frac{1}{\sigma_m^{N_m}\, 2^{N_m/2}\, \Gamma(N_m/2)} d_m^{N_m/2-1} e^{-d_m/2\sigma^2_m} \tag{7}$$

where $\Gamma(\cdot)$ is the Gamma function [11].

III. Receiver Processing

The UWB-IR system will take an action upon processing the decision variables $\{d_m\}$ given in (4). In the next four subsections, initially a general approach for receiver processing is presented for a single system and for multiple systems, followed by the presentation of two specific detection methods for multiple systems, which are the NP test for independent detection and the MAP criterion for joint detection.

A. Detection of a Single System

If the primary systems are independent, the decision variables obtained from each frequency band can be processed independently. To decide on the absence or presence of the mth primary system, the UWB-IR receiver compares the decision variable d_m to a pre-selected threshold value λ_m in order to take an action. The performance measures, probability

of false alarm and probability of detection, for the mth system can be expressed as

$$P_{f,m} = \Pr[d_m > \lambda_m | H_{0,m}] \quad (8)$$
$$P_{d,m} = \Pr[d_m > \lambda_m | H_{1,m}]. \quad (9)$$

Based on (7) both probabilities can be obtained as

$$P_{x,m} = \Gamma\left(\frac{N_m}{2}, \frac{\lambda_m}{2\sigma_m^2}\right) \Big/ \Gamma\left(\frac{N_m}{2}\right), \; x \in \{f, d\}, \quad (10)$$

with different σ_m^2 values for $H_{0,m}$ and $H_{1,m}$, where $\Gamma(\cdot\,,\cdot)$ is the incomplete Gamma function [11]. By adjusting the threshold value λ_m, desired $(P_{d,m}, P_{f,m})$ pairs can be obtained for given σ_m^2 and N_m values.

B. Detection of Multiple Systems

In the presence of multiple systems, the hypotheses have to be redefined. Initially, the set of hypotheses for M systems is defined as $\mathbf{H} = \left\{ \left[H_{x_M,M}, \ldots, H_{x_2,2}, H_{x_1,1}\right] | \, x_m \in \{0,1\} \right\}$ with 2^M possible options. We then define $\mathbf{H}_0 \in \mathbf{H}$, where $x_m = 0, \, \forall m$, for the case when no primary system is active, and $\mathbf{H}_1 \in \mathbf{H}$ for the remaining $2^M - 1$ cases when at least one system is active. This means that the UWB-IR system can safely transmit when $\mathbf{H}_0$ holds, and has to take precautions in the case of $\mathbf{H}_1$. We further define $\mathbf{H}_{1,i}$, $1 \le i \le 2^M - 1$, where

$$(i)_{10} = (x_M \cdots x_2 \, x_1)_2, \quad (11)$$

$(\cdot)_n$ is the logarithmic base n (e.g., $(3)_{10} = (1\,1)_2$ when $M = 2$), $\{x_m, \forall m\}$ refer to the subscripts of $\{H_{x_m,m}\}$, and $\mathbf{H}_1 = \bigcup_{i=1}^{2^M-1} \mathbf{H}_{1,i}$. Accordingly, the false alarm and detection probabilities for multiple systems can be redefined as

$$P_f = \Pr\left[P_{det} \middle| \mathbf{H}_0\right] \quad (12)$$
$$P_d = \sum_{i=1}^{2^M-1} \Pr\left[P_{det} \middle| \mathbf{H}_{1,i}\right] \Pr\left[\mathbf{H}_{1,i} \middle| \mathbf{H}_1\right] \quad (13)$$

where $P_{det} = 1 - \bigcap_{m=1}^{M} \Pr[d_m < \lambda_m]$.

We now introduce the joint system activity values $\{p_i \, | i = 0, 1, \ldots, 2^M - 1\}$, which provide information about the dependencies of the systems. We define $p_0 = \Pr\left[\mathbf{H}_0\right]$ as the probability that no primary system is active, and $p_i = \Pr\left[\mathbf{H}_{1,i}\right]$, $1 \le i \le 2^M - 1$, as the probability that $\mathbf{H}_{1,i}$ holds,[1] where $\sum_{i=0}^{2^M-1} p_i = 1$. Depending on the values of $\{p_i\}$, the activity and inactivity of the involved systems may be statistically dependent. This will be elaborated on in Section IV. To motivate our assumption on the system dependencies, we assume the presence of a system with uplink-downlink communications (i.e., $M = 2$). In the following, independent and joint detection methods are explained for such dependent systems.

[1] Accordingly, the corresponding active and inactive systems can be determined using the subscript of p_i in (11).

C. Independent Detection

In the case of independent detection, the decision variables $\{d_m\}$ will be compared to their corresponding threshold values $\{\lambda_m\}$ individually. When $M = 2$, P_f and P_d given in (12) and (13) become

$$P_f = 1 - \prod_{m=1}^{2} (1 - P_{f,m}) \quad (14)$$
$$P_d = 1 - \sum_{i=1}^{3} \frac{p_i}{1 - p_0} \prod_{m=1}^{2} (1 - P_{d,m})^{x_m} (1 - P_{f,m})^{(1-x_m)} \quad (15)$$

where $\{x_m\}$ can be obtained from (11) for a given i. In any DAA application, the detection method selected should maximize the detection probability for a target false alarm probability. For that reason, the NP test is employed, which optimizes the threshold values individually in order to maximize P_d for a given target $P_f = \alpha$. This can be formulated as

$$\max_{\lambda_1, \lambda_2} \; P_d \quad s.t. \; P_f = \alpha. \quad (16)$$

Using (8)–(10), (14) and (15) in (16), we obtain the best P_d values for target $P_f = \{\alpha\}$ values. This is achieved by expressing λ_2 and P_d as a function of λ_1, and by finding the λ_1 value that satisfies $\frac{\partial P_d}{\partial \lambda_1} = 0$. Due to space constraints, we are not able to provide the related derivation here. However, related plots will be presented in Section IV. As an alternative detection method, we will consider joint detection in the next section.

D. Joint Detection

Assuming that the systems' joint activity values $\{p_i\}$ and the pdf's of the decision variables $\{d_m\}$ are known, the MAP decision rule can be employed. Accordingly, the hypothesis can be estimated by finding the maximum of the MAP decision metrics as

$$\hat{i} = \arg\max_{i \in \{0,1,2,3\}} PM_i$$
$$\hat{\mathbf{H}} = \mathbf{H}_0 \text{ if } \hat{i} = 0; \quad \hat{\mathbf{H}} = \mathbf{H}_{1,\hat{i}} \text{ if } \hat{i} = \{1, 2, 3\} \quad (17)$$

where

$$PM_i = b_i \, p_i \, f_{D_1, D_2 | \mathbf{H}}(d_1, d_2), \quad (18)$$

$\{b_i\}$ are the intentionally introduced bias terms that are used to achieve a desired trade-off between the detection and false alarm probabilities, and $f_{D_1, D_2 | \mathbf{H}}(d_1, d_2)$ is the joint pdf of the decision variables d_1 and d_2 conditioned on the hypotheses. Since the decision variables are obtained from non-overlapping frequency bands, the pdf's of the variables are independent. Hence, the decision metrics, $\{PM_i \, | i = 0, 1, 2, 3\}$ can be simplified to

$$PM_i = b_i \, p_i \, C \prod_{m=1}^{2} \frac{\exp\left(\frac{-d_m}{2(\gamma_m + 1)^{x_m}}\right)}{(\gamma_m + 1)^{x_m N_m / 2}} \quad (19)$$

where $C = \prod_{m=1}^{2} \frac{d_m^{N_m/2-1}}{2^{N_m/2}\Gamma(N_m/2)}$ is the common term for $\forall PM_i$. Based on (17), the probabilities of false alarm and detection can be defined, respectively, as

$$P_f = 1 - \Pr\left[\bigcap_{i=1}^{3} \left(PM_0 > PM_i\right) \middle| \mathbf{H}_0\right] \quad (20)$$

$$P_d = 1 - \sum_{i=1}^{3} \frac{p_i}{1-p_0} \Pr\left[\bigcap_{j=1}^{3} \left(PM_0 > PM_j\right) \middle| \mathbf{H}_{1,i}\right]. \quad (21)$$

By substituting (19) into the comparison term $\{PM_0 > PM_i\}$, (20) and (21) can be simplified to

$$P_f = 1 - \prod_{m=1}^{2} (1 - P_{f,m}) \times \Pr\left[\sum_{m=1}^{2} d_m a_m < \lambda_3 \middle| d_1 < \lambda_1, d_2 < \lambda_2, \mathbf{H}_0\right] \quad (22)$$

$$P_d = 1 - \sum_{i=1}^{3} \frac{p_i}{1-p_0} \prod_{m=1}^{2} (1-P_{d,m})^{x_m} (1-P_{f,m})^{(1-x_m)} \times \Pr\left[\sum_{m=1}^{2} d_m a_m < \lambda_3 \middle| d_1 < \lambda_1, d_2 < \lambda_2, \mathbf{H}_{1,i}\right] \quad (23)$$

where $a_m = \frac{\gamma_m}{2(\gamma_m+1)}$ and $\lambda_m = \left[\frac{N_m}{2}\ln(\gamma_m+1) + \ln(\frac{p_0}{p_m}) + \ln(\frac{b_0}{b_m})\right]/a_m$ for $m = \{1,2\}$, and $\lambda_3 = \left[\sum_{m=1}^{2} \frac{N_m}{2}\ln(\gamma_m + 1) + \ln(\frac{p_0}{p_3}) + \ln(\frac{b_0}{b_3})\right]$. It can be observed that (22) and (23) have one additional term compared to (14) and (15). Accordingly, depending on the value of λ_3, both of the values in the (P_f, P_d)-pair obtained from (22) and (23) will be less than or equal to the values in the (P_f, P_d)-pair obtained from (14) and (15). This joint decrease in P_f and P_d values may result in a better ROC performance if the P_d value for joint detection is greater than the P_d value for independent detection for a fixed value of $P_f = \alpha$ in both cases.

In order to obtain the best ROC curve, the NP test can be used as in the independent detection case. Accordingly, P_d can be maximized by optimizing the threshold values $\{\lambda_1, \lambda_2, \lambda_3\}$ jointly for a target probability of false alarm, $P_f = \alpha$. This can be formulated as

$$\max_{\lambda_1,\lambda_2,\lambda_3} \quad P_d \qquad s.t. \quad P_f = \alpha. \quad (24)$$

Since λ_3 depends on the threshold values λ_1 and λ_2, it is not trivial to solve the numerical relation between P_d and the thresholds. Therefore, in this initial study, we investigate the ROC curves with empirically chosen values for the bias terms (see Section IV), $\{b_i\}$, in order to compare the joint and independent detection schemes. In the next section, the performances of the two detection schemes are compared for various scenarios.

IV. Results

In this section, initially the NP test based independent detection is verified, followed by a performance comparison between independent and joint detection. For performance evaluation, complementary ROC curves (i.e., P_f vs. $P_{md} = 1 - P_d$ (probability of missdetection)) are plotted. Complementary ROC curves are obtained by the NP test for independent detection and by varying the bias terms, $\{b_i\}$, for joint detection. For the bias terms, it is assumed that $b_1 = b_2 = b_3 = b$, therefore, the terms that contain the bias term, $\ln(\frac{b_0}{b_m})$, in λ_m $\forall m$ are equal, hence the complementary ROC can be generated by only varying b. For both detection schemes, it is assumed that the joint system activity values $\mathbf{p} = \{p_0, p_1, p_2, p_3\}$, the time-bandwidth products N_1 and N_2, and the SNR values γ_1 and γ_2 are known for the $M = 2$ active systems.

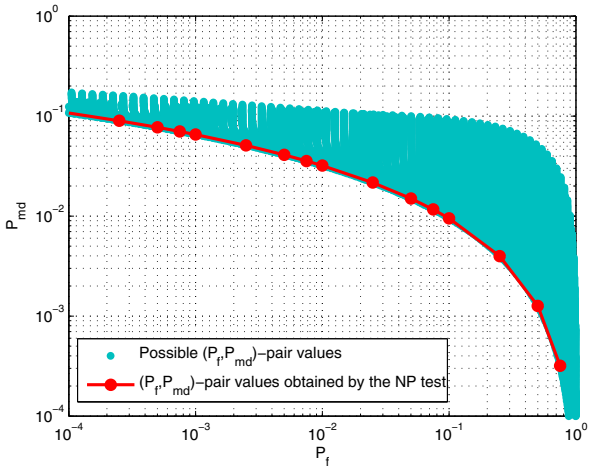

Fig. 1. The (P_f, P_{md})-pair search space and the (P_f, P_{md})-pairs obtained by the NP test when $\mathbf{p} = \{0.45, 0.25, 0.10, 0.20\}$, $N_1 = 12$ and $N_2 = 8$, and $\gamma_1 = 5$ dB and $\gamma_2 = 10$ dB.

In Fig. 1, the possible (P_f, P_{md})-pairs that can be obtained by using various λ_1 and λ_2 values in (14) and (15), i.e., the search space for independent detection, and the numerically calculated minimum P_{md} values for $P_f = \alpha$ fixed are plotted when $\mathbf{p} = \{0.45, 0.25, 0.10, 0.20\}$, $N_1 = 12$, $N_2 = 8$, and $\gamma_1 = 5$ dB, $\gamma_2 = 10$ dB. It can be observed that, as expected, the best (P_f, P_{md})-pairs are obtained by the NP test as the curve attains the lower bound of the search space.

In Fig. 2, complementary ROC curves are plotted for independent and joint detection when $N_1 = N_2 = \{4, 8, 12\}$, $\gamma_1 = \gamma_2 = 10$ dB and the two systems are active with either $\mathbf{p} = \{0.81, 0.09, 0.09, 0.01\}$ or $\tilde{\mathbf{p}} = \{0.90, 0.00, 0.00, 0.10\}$. The selection of $N_1 = N_2$ indicates that for two primary systems with the same bandwidth $W_1 = W_2$, the receiver integration time is selected as $T_1 = T_2$, which is a practical consideration. The first choice of $\mathbf{p}$ corresponds to the case when the two systems are independent from each other with each being active 10% of the time, and the second choice of $\tilde{\mathbf{p}}$ corresponds to the case when the two systems are *fully* dependent on each other. That is, the systems are simultaneously active 10% of the time and passive 90% of the time.

When $N_1 = N_2 = 4$ and $\mathbf{p} = \{0.81, 0.09, 0.09, 0.01\}$, independent and joint detection perform the same as observed in Fig. 2. When $N_1 = N_2 = 4$ and $\tilde{\mathbf{p}} = \{0.90, 0.00, 0.00, 0.10\}$,

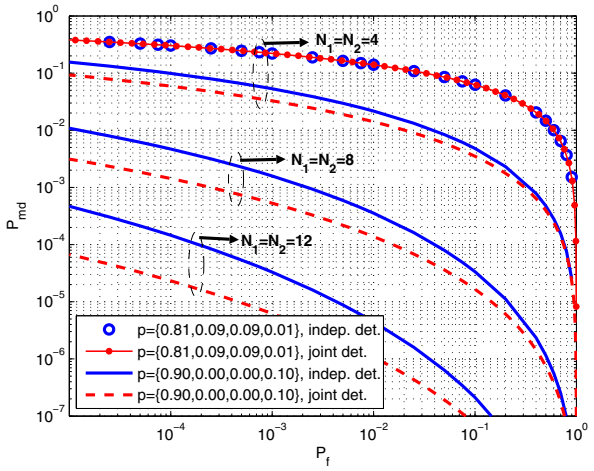

Fig. 2. Complementary ROC curves for independent and joint detection when $N_1 = N_2 = \{4, 8, 12\}$, $\gamma_1 = \gamma_2 = 10$ dB, $\mathbf{p} = \{0.81, 0.09, 0.09, 0.01\}$, and $\tilde{\mathbf{p}} = \{0.90, 0.00, 0.00, 0.10\}$.

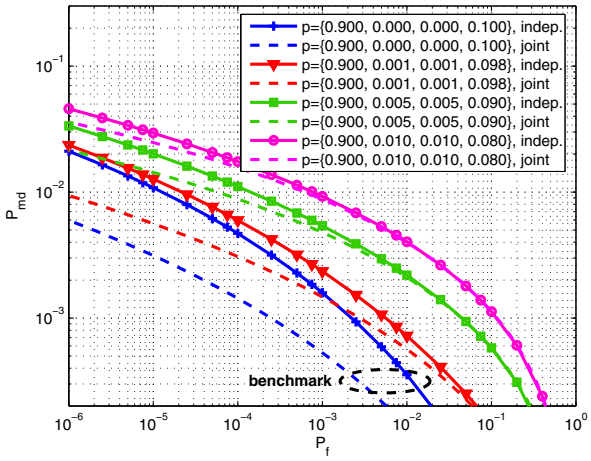

Fig. 3. The comparison of independent and joint detection for various $\mathbf{p}$ values when $N_1 = N_2 = 8$ and $\gamma_1 = \gamma_2 = 10$ dB.

the ROC performance for both detection schemes improves. This is due to both primary systems being active at the same time, and even if one of the systems is not detected, $\mathbf{H}_1$ would still hold. On the other hand, it is observed that joint detection outperforms independent detection for low values of P_f. To obtain a low P_f value, the threshold values of λ_1 and λ_2 should be high. Hence, selecting a low λ_3 value results in the last term of (22) and (23) being less than unity, which results in a trade-off in P_f vs. P_d performance. Thus, this can possibly provide a detection gain over independent detection when P_f is low. Finally, the effect of N_1 and N_2 on the detection gain is discussed. While a low P_f is *desired* in any DAA application (from the secondary system perspective), a low P_{md} is a *must* (from the primary system perspective). Accordingly, we can observe that P_{md} of joint detection becomes one half (when $N_1 = N_2 = 8$) and one fifth (when $N_1 = N_2 = 12$) of P_{md} of independent detection at $P_f = 10^{-3}$. Hence, it is important to select an appropriate integration time for fixed bandwidth systems to achieve a low probability of missdetection, where an increase in $N_1 = N_2$ results in lower P_{md} values for joint detection compared to independent detection. Although not plotted, a similar observation was made regarding the detection gain when the SNR was increased.

In Fig. 3, independent and joint detection are compared for various $\mathbf{p}$ values when $N_1 = N_2 = 8$ and $\gamma_1 = \gamma_2 = 10$ dB. The case when $\mathbf{p} = \{0.90, 0.00, 0.00, 0.10\}$ serves as a benchmark for the detection gain of joint detection over independent detection since the two primary systems are fully dependent. The common property of the $\mathbf{p}$ values in the legend of Fig. 3 is that they all satisfy $\Pr[\mathbf{H}_0] = 0.90$ and $\Pr[\mathbf{H}_1] = 0.10$. Accordingly, it is observed that the detection gain of joint detection decreases with decreasing p_3 values for $\Pr[\mathbf{H}_0] = 0.90$ and $\Pr[\mathbf{H}_1] = 0.10$ fixed.

V. Conclusion and Future Work

In this paper, we investigated the potential advantages of joint detection of multiple primary systems over independent detection when the systems were dependent and the dependence statistics were available. For that, the ROC performances of NP test based independent detection and MAP detection based joint detection were studied. A comparison of these detection schemes suggests that detection gain increases with dependence of the systems and for lower false alarm probabilities (i.e., when the threshold values are higher). This result is based on obtaining the *optimum* ROC curve using an NP test for independent detection and a *suboptimal* curve by varying a single bias value for joint detection. Therefore, the detection gain of joint detection is expected to increase with an optimum ROC curve and is subject to further investigation.

References

[1] IEEE Std 802.15.4a-2007, "Part 15.4: Wireless Medium Access Control (MAC) and Physical Layer (PHY) Specifications for Low-Rate Wireless Personal Area Networks (WPANs)," 2007.

[2] F. F. Digham, M.-S. Alouini, and M. K. Simon, "On the energy detection of unknown signals over fading channels," *IEEE Trans. Commun.*, vol. 55, pp. 21–24, Jan. 2007.

[3] A. Pandharipande and J.-P. M. G. Linnartz, "Performance analysis of primary user detection in a multiple antenna cognitive radio," *IEEE Proc. ICC '07*, pp. 6482–6486, June 2007.

[4] S. M. Mishra and R. W. Brodersen, "Cognitive technology for improving ultra-wideband (UWB) coexistence," *IEEE Proc. ICUWB '07*, pp. 253–258, Sep. 2007.

[5] K. Ohno and T. Ikegami, "Interference DAA technique for coexisting UWB radio," *IEEE Proc. VTC-Spring '07*, pp. 2910–2914, Apr. 2007.

[6] S. Erkucuk, L. Lampe, and R. Schober, "Analysis of interference sensing for DAA UWB-IR systems," *IEEE Proc. ICUWB '08*, vol. 3, pp. 17–20, Sep. 2008.

[7] Z. Quan, S. Cui, A. H. Sayed, and H. V. Poor, "Wideband spectrum sensing in cognitive radio networks," *IEEE Proc. ICC '08*, pp. 901–906, May 2008.

[8] Z. Quan, S. Cui, A. H. Sayed, and H. V. Poor, "Spatial-spectral joint detection for wideband spectrum sensing in cognitive radio networks," *IEEE Proc. ICASSP '08*, pp. 2793–2796, Apr. 4 2008.

[9] IEEE Std 802.16-2004, "Part 16: Air Interface for Fixed Broadband Wireless Access Systems," 2004.

[10] H. Urkowitz, "Energy detection of unknown deterministic signals," *Proc. IEEE*, vol. 55, pp. 523–531, Apr. 1967.

[11] M. Abramowitz and I. Stegun, Handbook of Mathematical Functions, Dover, New York, 1964.